universität wien

MASTERARBEIT / MASTER'S THESIS

Titel der Masterarbeit / Title of the Master's Thesis

Dissecting the progression of cardiac dysfunction in tumor-bearing mice

verfasst von / submitted by

Christopher Dostal, BSc

angestrebter akademischer Grad / in partial fulfilment of the requirements for the degree of

Master of Science (MSc)

Wien, 2022 / Vienna, 2022

Studienkennzahl lt. Studienblatt / degree programme code as it appears on the student record sheet:	UA 066 834
Studienrichtung lt. Studienblatt / degree programme as it appears on the student record sheet:	Masterstudium Molekulare Biologie UG2002
Betreut von / Supervisor:	Univ. Prof. Dr. Bruno Podesser

Acknowlegement

First of all I would like to thank and express my appreciation to my supervisors Dr. Attila Kiss and Prof. Dr. Bruno K. Podesser for their guidance and support in this project. Additionally, I would like to thank Prof. Dr. Erwin F. Wagner and his group including Dr. Latifa Bakiri, Dr. Casian-Simon Aioanei, Dr. Marta Dudek from the Medical University Vienna Genes and Disease group for collaborating with us.

I would also like to mention my collegues Lujza Szabo, Milat Inci, Eylem Acar, Shalett Matthew, Lukas Weber Maneesha Kururppu Appuhamilage, and Simge Baydar who supported me and showed me so many different techniques. Their company in the laboratory will always be remembered.

Very special thanks to Johanna Reiner for accepting my long working days in the laboratory and helping me proofreading my thesis.

Finally, I would like to thank my familiy and friends for constantly assisting me on my journy to become a scientist.

“If research was easy,

everyone would do it!”

Carl S. Apstein

Inhalt

Abstract

Background

Cancer patients undergoing heart-related complications result in high incidences of mortality. It is not understood whether tumors affect heart function prior to the onset of cachexia. In addition, we focus on expression of BCL-2–associated athanogene 3 (BAG3), a co-chaperone protein and Hsp70, which are highly expressed in tumors but decrease in cardiomyocytes in heart failure.

Methods

Colon-26 adenocarcinoma cells (C26; n=22) with/without shIL-6 (C26 shIL-6; n=22) were injected subcutaneously of 10-11 weeks old BALB/c male mice. Controls were injected with vehicle (PBS; n=8). Cardiac function was assessed by echocardiography and invasive hemodynamic measurements 10 and 20 days after the injection. In addition, the expression of BAG3 and Hsp70 were determined by Western blot.

Results

Only C26 group showed a significant loss of subcutaneous fat and skeletal muscle ($p<0.05$, respectively), suggesting cachexia. Left ventricular ejection fraction (LVEF) showed a tendency to decline in the early phase ($p\sim0.08$) in both injected groups and it reached significance at the late stage ($p<0.05$). Hemodynamic assessment confirmed a decrease in LV systolic pressure and increase of LV end-diastolic pressure ($p<0.05$, respectively). These heart related changes were associated with a marked reduction in both BAG3 and Hsp70 in the myocardium.

Discussion

Our study shows for the first time that tumors play a significant maladaptive role in the progression of cardiac dysfunction in a mouse model of C26 injection-induced cachexia. The progression of cardiac contractile dysfunction was associated with a decline in BAG3 and Hsp70 in tumor-bearing mice, suggesting changes of BAG3/Hsp 70 signalling may be a critical component.

Background

Cancer patients undergoing heart-related complications result in a high incidences of mortality [1]. Nevertheless, it is still not fully understood whether localized tumors affect the heart function before the onset of end stage of the diseases and cachexia, hence, making the heart more vulnerable to functional abnormalities in later stages of the disease [2-4]. It is still largely unknown what signaling mechanisms, mediators and which effectors contribute to both cardiac and vascular dysfunction among cancer patients. Thus, for analyzing the heart function, we focus on the expression BCL-2–associated athanogene 3 (BAG3), a co-chaperone protein and Hsp70, which is highly expressed in tumor cells but decreases in cardiomyocytes (CM) in various forms of heart disease [5-9].

Heart

In brief, the heart main function is to pump oxygenated blood through the vasculature and provide thereby a flow of nutrition and oxygen to every tissue in the body. Cardiovascular diseases (CVD) are a group of heart and small or larger vascular beds related disease and substantially contribute to mortality and hospitalization. They are one of the leading causes of death [10] besides cancer in the western world. CVDs are often chronic and many risk factors lead to progression of CVD, most commonly hypertension and hyperlipidemia [10]. Cardiac dysfunction and the risk of developing heart failure (HF) are well-known side-effects of chemotherapeutic treatment in cancer survival patients [1].

Cancer

Cancer is the leading cause of death worldwide. One of six deaths are related to cancer, over 10 million deaths in 2020, accordingly to the World Health Organization. Cancer is not just one disease, based on the tissue that is affected, different types are known [11]. Cancer is also associated with cardiomyopathy and leads to many expression changes in cardiac tissue. Cancer also leads to Cancer-Associated Cachexia, which as well affects the heart [4, 12, 13]. Cardiac remodeling vice versa showed negative effects on

metastasis and cancer cell proliferation, which leads to faster cancer growth [14].

Cancer-Associated Cachexia

Cancer-Associated Cachexia (CAC) is a metabolic state of energy waste that affects the whole body and is characterized by a loss of adipose tissue, muscle tissue, and systematic inflammation [15]. In contrast to other causes of Cachexia, CAC is strongly associated with cancer, unlike other forms of cachexia, which can be related to heart failure, malnutrition, or patients with HIV. In any case, cachexia is a severe complication and treatment is limited [16-19]. Cancer-Associated Cachexia has to be established first to be then maifested. It is distinguishable in an early and late stage. In the early phase, loss of adipose tissue can be measured, later adipose tissue and muscle reduction is prominent [20]. Weight loss is associated with a poor prognosis in cancer patients and affects their morbidity [21, 22]. Additionally, C26 (colon-26-adenocarcinoma) cells injected into Balb/c mice treated with monoclonal antibody against murine IL-6 resulted in significant less muscle and fat wasting [23]. Furthermore, IL-6 as a target in cancer/cachexia therapy is discussed in different types of cancer [24]. Interestingly, some IL-6 gene polymorphisms are associated with higher risk of cachexia and lower survival rate in patients with pancreatic cancer [25]. Overall, IL6 depletion is a great tool for studys concentrating on effects of cancer-associatet cachexia.

Cardiac remodeling in cancer-associated cachexia

Structural and functional changes of the heart are a hallmark of HF. Cardiac remodeling the process of adaptation of the heart to pressure or volume overload conditions, is by the definition not a malign process, so under physiologic condition e.g training, hearts start to adapt to the exercise [26]. Beside the physiological process, hearts can also adapt in a malign way as responds to different conditions e.g. Ischemia, pressure overload, volume overload, this is associated with an increase in collagen accumulation, fibrosis and cardiomyocyte contractile function [14, 27]. A recent study demonstrated that mice in which a transverse aortic constriction to develop LV hypertrophy,

was performed, are prone to metastasis and show higher cancer growth [14]. Additionally, under cancer-associated cachectic conditions different changes in gene expression occur, 268 cardiac genes are differently expressed in C26 tumor bearing mice [28], proteomic approaches identified 24 different expressed cardiac proteins in these mice [13]. Subsequently, tumor bearing mice showed under cancer-associated cachexia increased collagen deposits in the left ventricle, declined cardiac myofibriles [29], changes in the extracellular matrix, cardiac fibrosis, and increased ubiquitination of cardiac proteins, which leads to increased degradation and loss of heart mass [30]. NF-κB pathway is also a factor in systolic dysfunction and atrophy of tumor bearing mice suffering cancer-associated cachexia [31]. Another study showed that oxidative damage to DNA is associated with cardiac athropy [32].

Overall, it is not known which changes are cancer linked and which are a result of cancer-associated cachexia. Generally, it is still unclear in which mechanisms cancer-associated cahexia and cardiac dysfunction are involved in.

BCL-2–associated athanogene 3 and Hsp70

Bag3, a co chaperon of Hsp70, is known for several key processes in cell function and metabolism. In cancers, Bag3 expression upregulates and linkes to more proliferation of cancer cells [33]. In contrast, alterations of Bag3 in the heart are associated with hypertrophic and dilated cardiomyopathy [33]. Mutations of Bag3 lead to Z-disc disintegration and aggregation of proteins [6]. Additionally, decreased levels of Bag3 were found in end stage HF in humans and in murine models of ischemic HF [7]. Moreover, it is known that Bag3 regulates myofilament contractile and Ca^{2+} homeostasis in cardiomyocytes, so this suggests that dysregulation of Bag3 expression may play role in arrhythmogenesis [5].

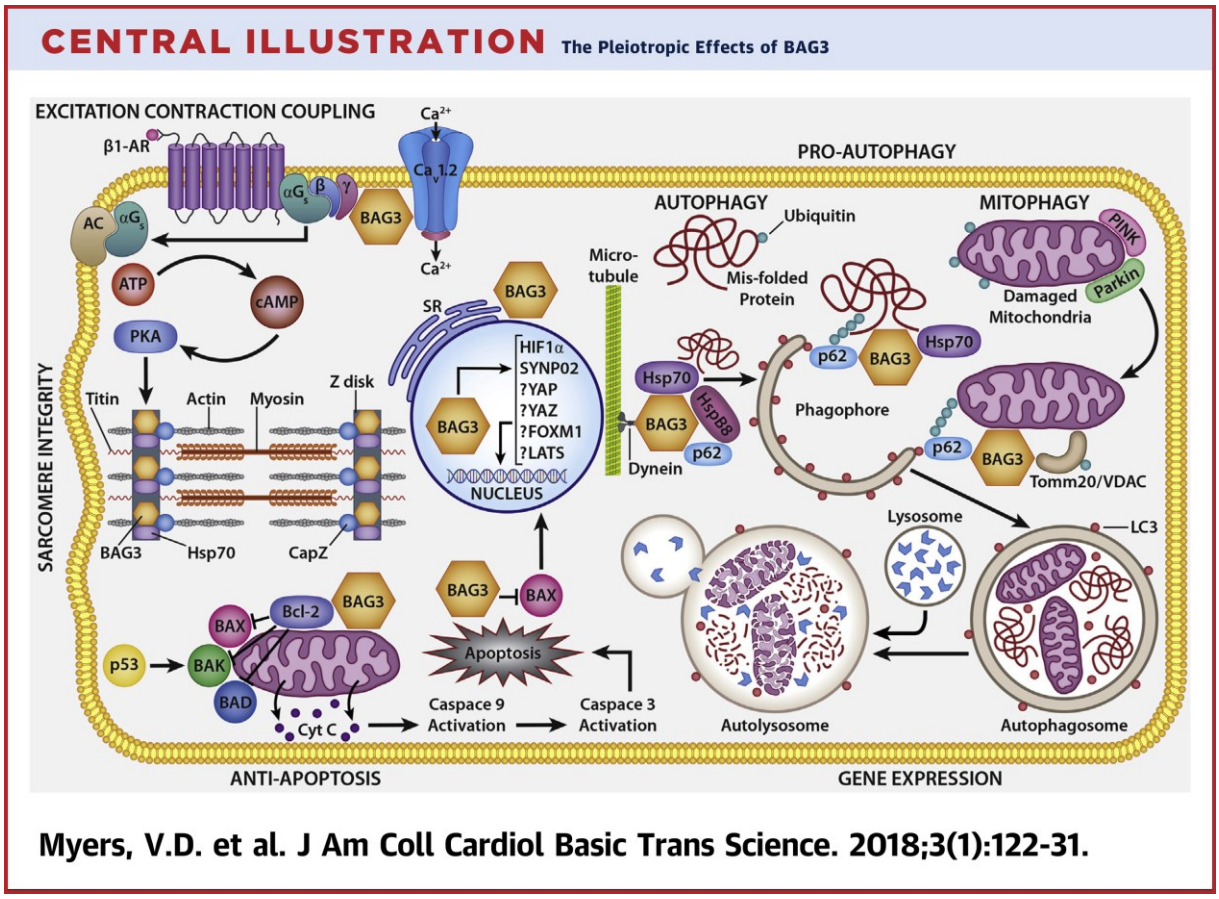

Myers, V.D. et al. J Am Coll Cardiol Basic Trans Science. 2018;3(1):122-31.

Fig 1: The major pathways of BAG3 function in the heart illustrated by Myers, V.D et al. [33]: autophagy, apoptosis, maintenance of adrenergic responsiveness and excitation–contraction coupling, support of the sarcomere, and modulation of gene expression. Abbreviations used by Myers, V.D., et al. in this figure: αG_s = alpha subunit of the guanine nucleotide binding protein; β_1-AR = β_1-adrenergic receptor; AC = adenylyl cyclase; ATP = adenosine triphosphate; BAD = B-cell lymphoma-2–associated death; Bax = B-cell lymphoma-2–associated X protein; BAK = B-cell lymphoma-2 homologous promoter; antagonist/killer; Bcl-2 = B-cell lymphoma-2; cAMP = cyclic adenosine monophosphate; Ca_v-1.2 = L-type Ca^{2+} channel; Cyt C = cytochrome C; FOX M1 = Forkhead box 14 M1 transcription factor; HIF 1α = hypoxia-inducible factor 1 active transcription factor; LATS = serine/threonine protein kinase; LC3 = microtubule-associated protein 1A/B-light chain 3; p53 = tumor suppressor protein; SR = sarcoplasmic reticulum; PKA = protein kinase A; SYNPO2 = protein coding gene synaptopodin 2; Tomm20 = mitochondrial import receptor subunit TOM20 homolog; VDAC = voltage-dependent anion channel; YAP = yes-associated transcriptional regulator; YAZ = transcription factor.

To an different aspect, Bag3 promotes autophagy of small heat shock proteins. Furthermore, Bag3 acts in general as a regulator of protein degradation, this mean that overexpression of Bag3 can lead to autophagy of myocardial proteins [34]. However, under stress conditions, cardiomyocytes accumulate Hsp70 on the cell membrane and serum. Isolated cardiomyocytes react to recombinant Hsp70 with reduced contractility and increased apoptosis [35]. A recent study showed that Bag3 could promote physiological hypertrophy and could prevent pathological remodeling by activation of the AKT/mTOR pathway [9]. Bag3

seems to be important for reducing apoptosis of cardiomyocytes, protein homeostasis, mitochondrial stability, contractility and cardiac arrhythmia. Overall it plays a significant role in cardiac protection and is an important target for our cancer-associated cachexia study [36]. Finally, Fig 1 depicts the many known pathways of Bag3 which was illustrated by Myers V.D. et al. [33].

AIM of Thesis

To conclude the already existing findings on cancer-associated cachexia and link to cardiac dysfunction. Nevertheless, it is still not fully understood whether localized tumors affect heart function before the onset of cachexia, hence, making the heart more vulnerable to functional abnormalities in later stages of the disease. Therefore, our study dissected the impact of cachexia or tumors on the progression of cardiac contractile dysfunction in mice.

Methods

Animal model

Colon-26 adenocarcinoma cells (10^6 C26; n=22) with/without shIL-6 (10^6 C26 shIL-6; n=22) were injected subcutaneously into the right flank of 10–11 weeks old BALB/c male mice. Silencing IL-6 in C26 cells leads to mild or even low levels of cachexia [23]. Control mice were injected with vehicle (PBS; n=8). With respect to early cachexia and late cachexia, two timepoints were chosen, namely, 10-11 and 20 days post injection. At the early time point, we anticipated animals to be normal weighted. However they were already in pre cachexia condition [2], the late timepoint was chosen accordingly to animal welfare protocols and to minimize animal suffering.

Transthoracic echocardiography

Mice were pre-anesthetized with 4-5% Isoflurane and placed on a heated stage. During the analysis, mice were monitored and continually anesthetized with 1-1.5% of Isoflurane. Imaging was performed using a Vevo 3100 System (Fujifilm, VisualSonic) equipped with a 25–55 MHz MX550D transducer. Left ventricular ejection faction (LVEF), left ventricular end-diastolic diameter (LVEDD) and left ventricular end-systolic diameter (LVESD) were evaluated at mid-papillary short-axis view and used as surrogate paramters for cardiac function as described previosuly [37].

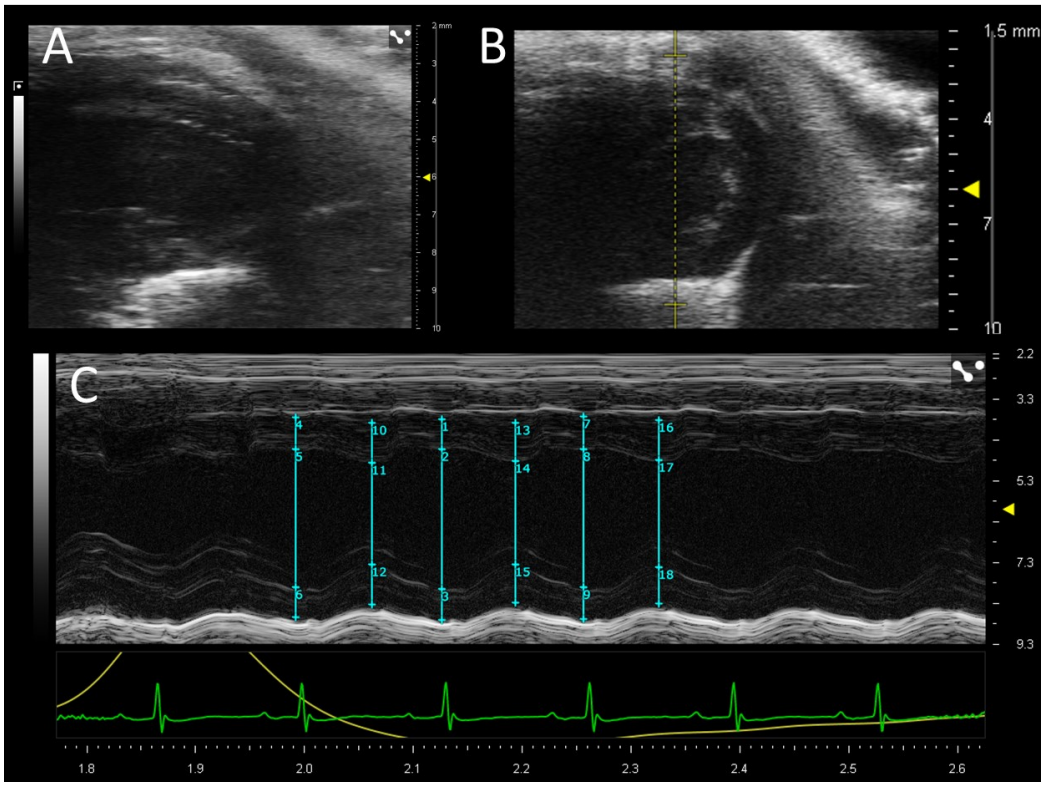

Fig 2: A) Representative echocardiography Long-axis view B) short-axis view with line marking the M-mode measurement C) M-mode, 3 consecutive measurements of systolic and diastolic diameters in short-axis

Left ventricular hemodynamic measurements

One to two days after the echocardiography measurement, mice were anesthetized with a mixture of xylazine (4mg/kg, Bayer, Germany) and ketamine (100mg/kg body weight, Dr. E. Gräub AG, Switzerland, i.p.) Mice were mechanically ventilated then lateral cutting was performed to open the abdominal cave, a microscissor was used to open the diaphragm and a microtip catheter (1F, Millar Instruments, Houston, TX, USA) was placed in the LV through the apex of the heart. Hemodynamic parameters were continually monitored with LabChart (v7.3.2) and PowerLab System (8/30; ADInstruments, Spechbach, Germany). After measurement, the organs were removed and put into cold Krebs-Henseleit Buffer. Blood samples were used for serum preparation. Organs were weighted, including heart, lung, spleen, kidney, white adipose tissue, and brown adipose tissue (BAT). White adipose tissue (WAT) was split based on region into inguinal WAT (iWAT), gonadal WAT (gWAT), abdominal WAT (aWAT). Organs were snap frozen, exception of the hearts, which were cut in half on mid papillary levels then to fix in PFA, the apical part was snap frozen.

Isolation of endothelial cells from the Lungs

The lungs were placed in cold PBS and cut into smaller segments. The segments were put into 37°C warm Collagenase Type I PBS solution (2mg/ml) and incubated for 45 minutes at constant temperature. A cell strainer with 70 µm pores was used and erythrocytes were eliminated by red blood cell lysis buffer (Roche). To collect and isolate CD31+ cells, sheep anti-rat IgG coated Magnetic beads (Dynabeads, Invitrogen) were incubated and continuously shook on a shaking plate with rat anti-mouse CD31 IgG at 4°C overnight (25 µl Dynabeads and 2.5 µl CD31 antibody in 1 ml 0.1% PBS-BSA). The prepared beads and lung endothelial cell suspension were incubated for 20 minutes on a shaking plate at room temperature. Subsequently, the separation was done with three washing steps using a magnetic particle concentrator (Dynabeads, MPC-1 Magnets) and the cells lysate was stored for further analysis.

Angiotensin-converting enzyme 1 (ACE1) activity measurement

Tissue samples were cut and weighted, approximately 50–100 mg tissue was used for the measurement. Accordingly to the weight of tissue, for each mg 1 µl of 100 mM tris (hydroxymethyl) aminomethane hydrochloride (TRIS) buffer (pH 7.0) was added and homogenized. This was followed by a centrifugation step for 5 min at 15.000g. The supernatant was further used and transferred in a new Eppendorf tube to determine the protein concentration with a BCA Protein Assay Kit (Thermo Fisher Scientific) using a TECAN (SparkControl Magellan V2.2) plate reader. To determine the ACE activity, an artificial substrate (Abz-FRK(Dnp)P-OH, Enzo Life Sciences) was used in a reaction mixture containing 6 µl of 1 mg/ml tissue homogenates in 35-fold dilution in 100 mM TRIS buffer, 50 mM NaCl, 10 µM $ZnCl_2$. The intensity of the fluorescence signal and its changes were measured by TECAN (SparkControl Magellan V2.2) plate reader (excitation, 340 nm; emission, 405 nm) on 94 well plates (Greiner-Bio One) at 37°C). Enzymatic activity was measured for at least 30 circules (30 minutes) and the data was plotted as a function of reaction time. Additionally, linear regression of the fluorescence intensity values was performed by GraphPad (GraphPad Software, San Diego, CA, USA) and the fit was only accepted when r2 was >0.9. To calculate the ACE activity, the following equation was used:

$$activity = \left(\frac{S}{k}\right) * \frac{D}{P}$$

where S represents the increase in the fluorescence intensity (1/min) and k is the change in Fluorescence intensity during the complete cleavage of 1 pmol Abz-FRK(Dnp)P-OH substrate. D represents the dilution of the sample and P the protein concentration in mg/ml.

Western Blot

BioRad Mini-Protean cells were used along with 10% Acrylamid/Bis-acrylamid (30:0,8) gels and separation buffer (TRIS 1.5 M, 0,4% SDS, pH 8.8) and stacking buffer (TRIS 0.5 M, 0,4% SDS, pH 6.8). Proteins were boiled in FSB/DTT buffer (100mM DTT) for up to 10 minutes and finally loaded onto the gel. The gel was run accordingly to BioRad at 100 Volts constant for 35 minutes. For semi-dry blotting, 3 Whatmann 3MM paper layer than the nitrocellulose membrane followed by the separation gel and another 3 layers of Whatmann 3MM papersare stacked and put into a Trans-Blot® Turbo™ Transfer Starter System for 30min. After blotting the membrane, it was incubated and washed several times with milk powder 5% dissolved in TTBS. Additionally, incubation with primary antibody BAG3 (E7Y9T) Rabbit mAb #23842 and HSP70 #4872 Rabbit Antibody from Cell Signalling with 1:1000 dilution in TTBS + 0.2M NaCl) overnight at 4°C and secondary antibody (Amersham ECL Anti-rabbit IgG, HRP-Linked Species-Specific Whole Antibody from donkey with 1:10000 dilution) was performed for 2h at room temperature followed by several washing steps. Subsequently, the membrane was covert with an equal amount of stable Peroxide Solution and Luminol Enhancer Solution and after 5 minutes of incubation the membrane was put into a transparent sheet and exposed to ECL-film Membrane staining with ponceau S (Ponceau S 0.2%,TCA 3%) was performed to quantify and evaluate the loaded protein bands.

RT-qPCR

For extracting RNA and miRNA out of the cell suspension a miRNeasy Mini Kit (Qiagen, Hilden, Germany) was used. Heart tissue was homogenized with a tissue rupture (Qiagen) with added QIAzol. Chloroform was added and then

centrifuged. Absolute ethanol was put on the upper phase, which was transferred to a miRNeasy Mini spin column. After washing the RNA, it was obtained by adding 30 µl nuclease-free water and collected with a final centrifugation step. The RNA concentration was measured using NanoQuant plateTM and TECAN plate reader (SparkControl Magellan V2.2) and cDNA was generated using a QuantiTect reverse transcription kit (Qiagen). After generating cDNA out of RNA, quantitative PCR was performed using a QuantiTect SYBR Green PCR kit (Qiagen). Duplicates were used and analysis was performed on ROTOR-Gene Q (Qiagen), gene expression was calculated by $2^{-\Delta\Delta CT}$ method [38].

Vascular reactivity assessments

Aorta abdominalis was collected (terminal sacrification) and was cut into 2 mm segments and cleaned from connective tissue in the cold Krebs-henseleit buffer (KHB) containing 119 mmol/l NaCl, 4.7 mmol/l KCl, 2.5 mmol/l $CaCl_2$, 1.17 mmol/l $MgSO_4$, 20 mmol/l $NaHCO_3$, 1.18 mmol/l KH_2PO_4, 0.027 mmol/l EDTA and 10.5 mmol/l glucose. Segments were flushed with KHB and put into a DMT Wire-myograph (Model 620 M, Danish Myo Technology, Aarhus, Denmark). Aortic segments were mounted on two 200 µm needles in a heated organ chamber. One needle is connected to a force transducer and the other one is connected to a micrometer screw to adjust the distance and stretched every minute 30-50µm until a calculated resting tension of 13.3 kPA is reached. To calculate, LabChart was used with the DMT module installed. After reaching the resting tension, the segments were equilibrated for 30 minutes followed by a contraction check with high potassium KHB (124 mM, KCl) for 3 min. The segments were flushed afterwards and equilibrated again for 20 min.

Vascular constriction assessment

Phenylephrine (Phe, Sigma-Aldrich) was added in concentrations steps of 1 nM to 10 uM and in cumulative dosage and plateau force were recorded for each step. Phenylephrine contraction was calculated in relation to the reached peak of high potassium KHB.

Endothelial function assessment

Acetylcholine (ACh, Sigma-Aldrich) was added in cumulative dosage in the range of 1 nM to 10 µM after adding Phe (conc). Vascular relaxation was continuously recorded via LabChart. Subsequently, organ chambers were washed with KHB and equilibrated for 20 minutes. Additionally, sodium nitroprusside (SNP, Sigma-Aldrich, 0.1 nM to 1 µM) was used to determine the endothelial-independent vasorelaxation.

Blood analysis

Blood analysis was performed with a point of care diagnostic scil Vet abc Plus (scil animal care company GmbH, Viernheim, Germany) and 10µl were used for animal blood analysis. The following values were measured; leukocytes (WBC), red blood cells (RBC), platelets (PLT), hemoglobin (HGB), hematocrit (HCT), Mean corpuscular volume (MCV), mean corpuscular hemoglobin (MCH), Mean corpuscular hemoglobin concentration MCHC, Red blood cell distribution width (RDW), mean platelet volume (MPV), and count of lymphocytes, monocytes, and eosinophiles, including their percentual distributions.

Histology

Mid-papillary heart tissue was fixed in formalin and paraffin-embedded and stained with Hemotoxylin/Eosin. Fibrosis staining was performed by a Masson-Goldner staining (Masson-Goldner staining kit, Sigma-Aldrich/Merck, Darmstadt, Germany). For imaging, a camera mounted to a microscope was used (VS120 Virtual Slide Microscope System, Olympus, Tokyo, Japan) with (AVT PIKE F-505C VC 50, Allied Vision Technologies, Stadtroda, Germany) attached. To assess the level of fibrosis, right and left ventricular areas of fibrosis were analysed with Adobe Photoshop Element (version 14.1) and the fibrotic area was set in relation to the non-fibrotic area.

Statistics

Prism GraphPad 8.0.1 (GraphPad Software, San Diego, CA, USA) was used for statistical analysis. Students T-Test was used for comparing of two Groups and oneway-ANOVA if more than two groups were used when they were metric and showed normal distribution. A significant difference was set to p-value less than 0.05 and data are presented as mean±SEM.

Results

Cachectic progression parameters

Bodyweight, white adipose tissue (WAT), brown adipose tissue (BAT), and m. Quadriceps, m. Gastronemius, and m Soleus was weighted. Mice with cachexia showed a significant decline in WAT, BAT, and muscle tissue. In contrast, silencing of IL-6 in C26 cells leads to mild or even low level of cachexia, even though the tumor size was not changed (Fig 3).

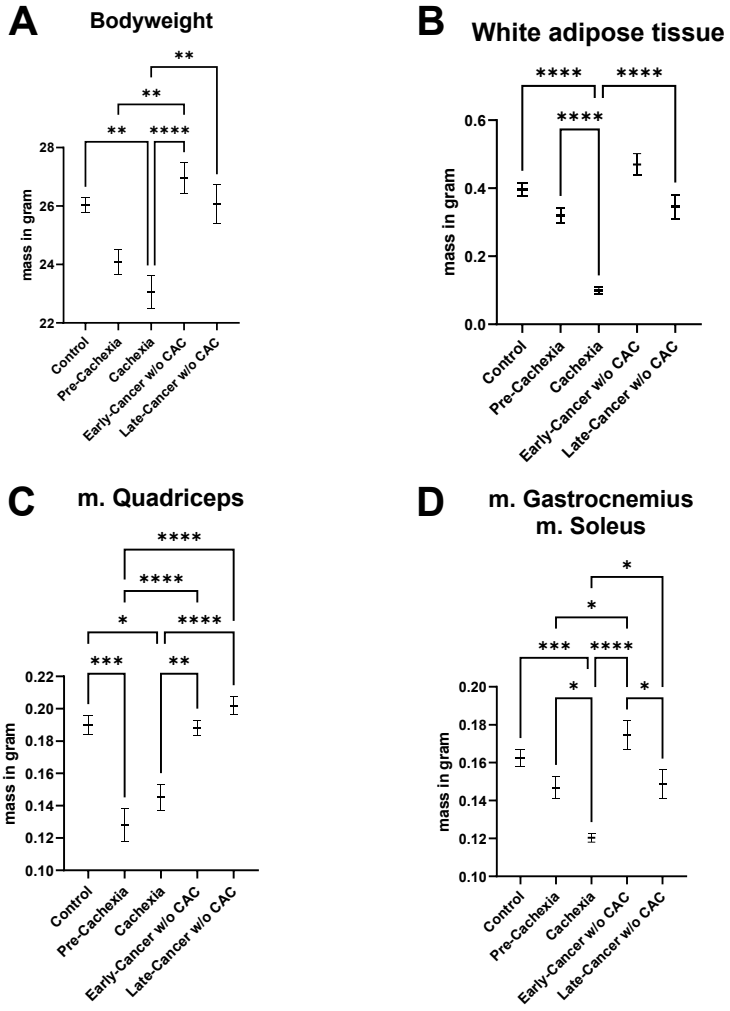

*Fig 3: A) Changes in body weight B) mass of white adipose tissue (WAT) changes and C) weight of musculus Quadriceps and D) weight of m. Gastrocnemius and m. Soleus. Mean±SEM, n=8 Control, n=11 Pre-Cachexia, n=11 Early-Cancer w/o CAC, n=12 Cachexia, n=10 Late-Cancer w/o CAC, *p<0.05,**p<0.01,***p<0.001, ****p<0.0001.*

Tumors were weighted and the mass of the other organs was determined as well. Interestingly, splenomegaly was observed in association with cachexia, while tumor bearing mice without cachexia showed splenomegaly only in the late stage (Fig 4). Total blood was taken and analyzed. The increase of neutrophile to lymphocyte ratio is a prognostic cancer marker [39]. The numbers and percentages of lymphocytes, granulocytes, and monocytes in the blood were markedly changed in tumor bearing mice. For mice with cachexia, these changes occurred earlier when compared to non-cachetic mice (Fig 4) .

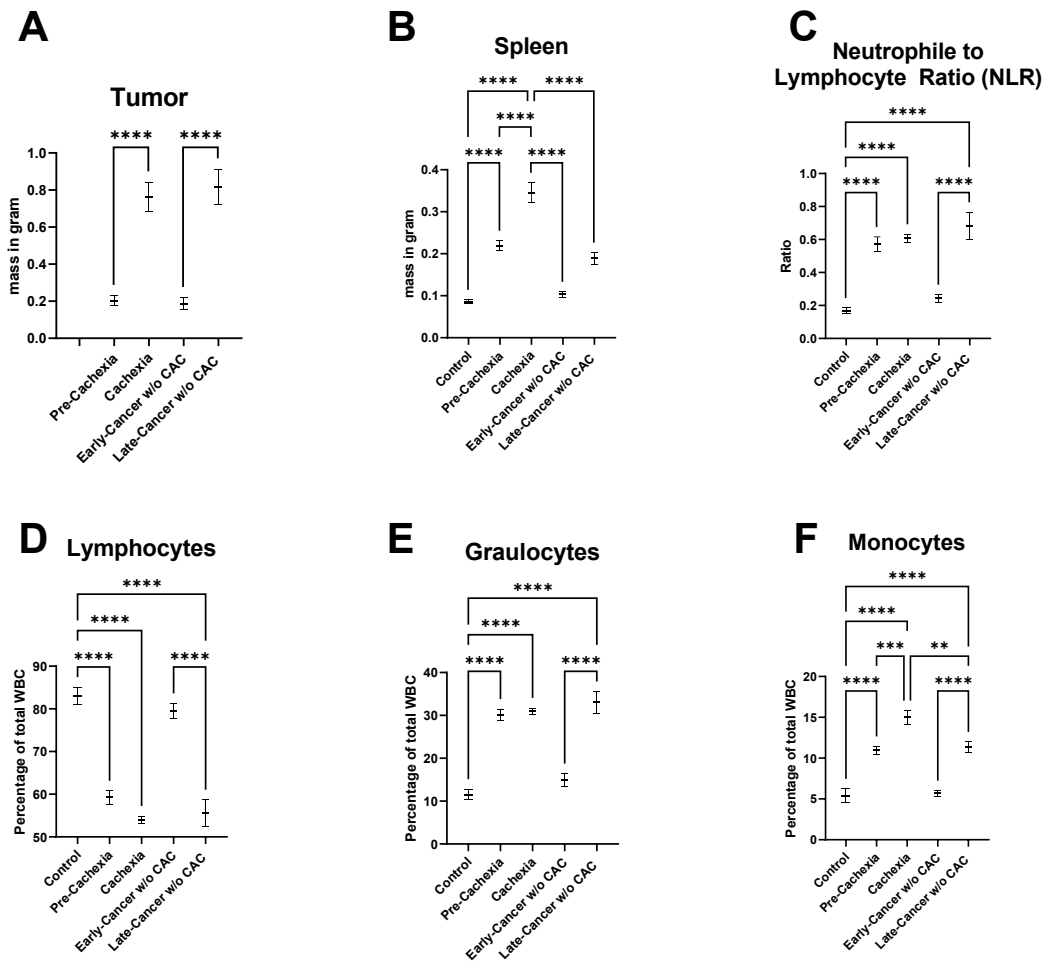

*Fig 4: A) tumor size B) spleen mass changes compared to controls C) neutrophil to lymphocyte ratio D, E, F) changes in lymphocytes (Lym), Granulocytes (Gra), and Monocytes (Mon) percentage of total white blood count. Mean±SEM, n=8 Control, n=11 Pre-Cachexia, n=11 Early-Cancer w/o CAC, n=12 Cachexia, n=10 Late-Cancer w/o CAC, *p<0.05,**p<0.01,***p<0.001, ****p<0.0001.*

Transthoracic Echocardiography

Transthoracal Echocardiography was performed one day before invasive hemodynamic measurement and under isoflurane anesthesia. Left ventricular ejection fraction (LVEF) was calculated from the common formula for ejection faction (EF):

$$EF\% = \frac{\text{enddiastolic volume} - \text{endsystolic volume}}{\text{enddiastolic volume}} * 100$$

We did not observe any significant difference between cachectic and non-cachectic animals in heart dimensions systolic or diastolic diameters. Nevertheless, LVEF is a surrogate end-point functional parameter of LV function. We observed that mice with tumors showed a significant reduction in LVEF in comparison to the controls (Fig 5). Additionally, non-cachectic animals showed a tendency toward to decline in LVEF in the early time point without statistical significance. Moreover, non-cachectic animals differ significantly in the late and early stage (Fig 5).

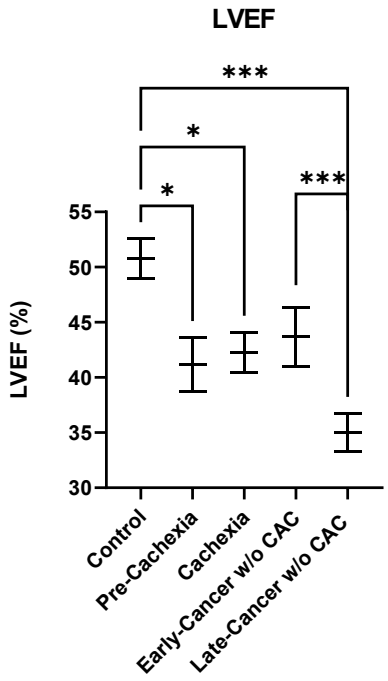

*Fig 5: Changes in left ventricular ejection fraction (LVEF) in between time point and cachectic as well non-cathectic tumor bearing mice compared to control animals. Mean±SEM, n=11 Control, n=14 Pre-Cachexia, n=14 Early-Cancer w/o CAC, n=12 Cachexia, n=10 Late-Cancer w/o CAC, *p<0.05,***p<0.001.*

Left ventricular hemodynamic measurements

Invasive hemodynamic measurement was performed 1–2 days after the echocardiographic assessment. The animals were deeply anesthetised with the mixture of ketamin/xylazine. Left ventricular systolic pressure was preserved in an early time point in tumor bearing mice when compared to controls. In contrast, we observed a significant decline in LVSP at the late stage of cancer/cachexia (Fig 6). Left ventricular diastolic dysfunction, LVEDP was increased in mice with tumors in comparison to control animals (Fig 7).

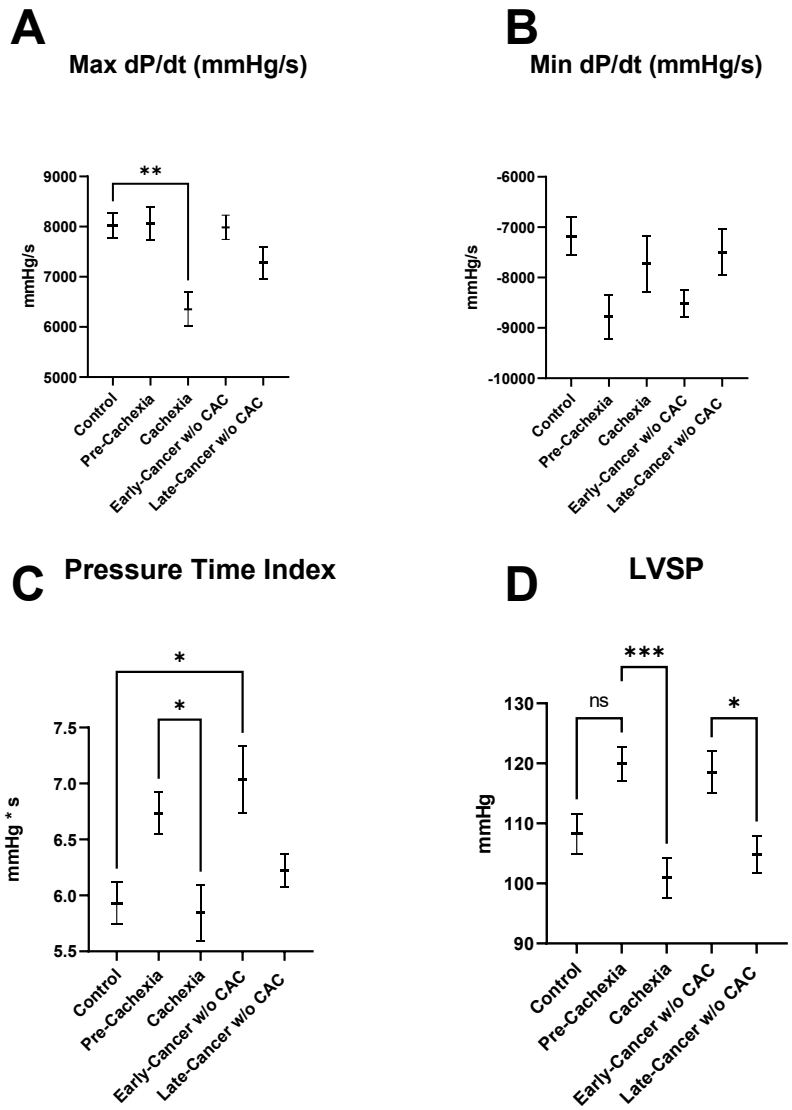

*Fig 6: A) Contractility differences in cachectic animals compared to controls B) diastolic function C) Pressure Time Index, average ventricular pressure during systole, multiplied by the systolic duration, changes in cachectic and early non-cachectic animals compared to controls D) LVSP change in early time point vs late tumor bearing mice. Mean±SEM, n=8 Control, n=11 Pre-Cachexia, n=11 Early-Cancer w/o CAC, n=11 Cachexia, n=10 Late-Cancer w/o CAC, *p<0.05,**p<0.01,***p<0.001.*

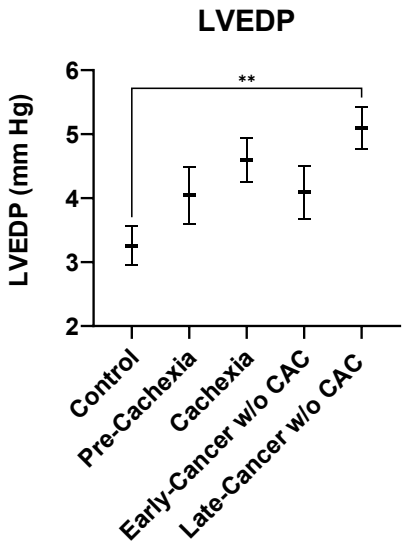

*Fig 7: LVEDP increased in late tumor bearing mice compared to controls, Mean±SEM, n=8 Control, n=11 Pre-Cachexia, n=11 Early-Cancer w/o CAC, n=11 Cachexia, n=10 Late-Cancer w/o CAC, *p<0.05,**p<0.01,***p<0.001.*

Vascular reactivity and stiffness

Vascular stiffness, was measured as the change in the intraluminal pressure in response to stretching of the vessel wall. Interestingly, the slope of the curve was increased already in an early timepoint in cachectic animals compared to control animals (Fig 8). In additon, the vascular stiffness was also increased in both tumor bearing mice at the late timepoint (Fig 8).

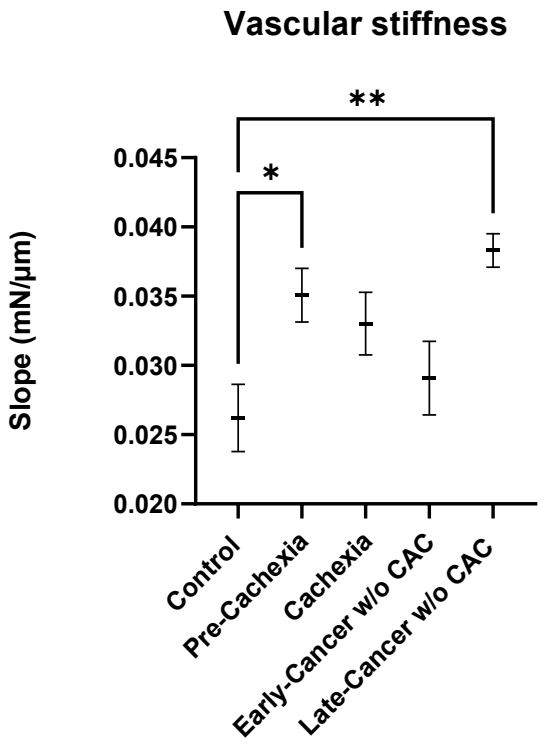

*Fig 8: Vascular stiffness calculated using mN change according to distance vessel is stretched. The slope increases in early cachexia and late tumor bearing mice. Mean±SEM, n=8 Control, n=4 Pre-Cachexia, n=4 Early-Cancer w/o CAC, n=4 Cachexia, n=4 Late-Cancer w/o CAC, *p<0.05,**p<0.01.*

Endothelial depending vascular reactivity was assessed by the response to the cumulative dosage of ACh. We observed that EC50 values of ACh was markedly increased in cachectic animals ($p<0.05$) (Fig 9). The contraction to the highest Phe concentration was on the same level in all groups, but again changes in LogEC50 can be observed and cachectic animals have lower EC50 values than non-cachectic tumor bearing mice. Relaxation to SNP showed no difference between the experimental groups.

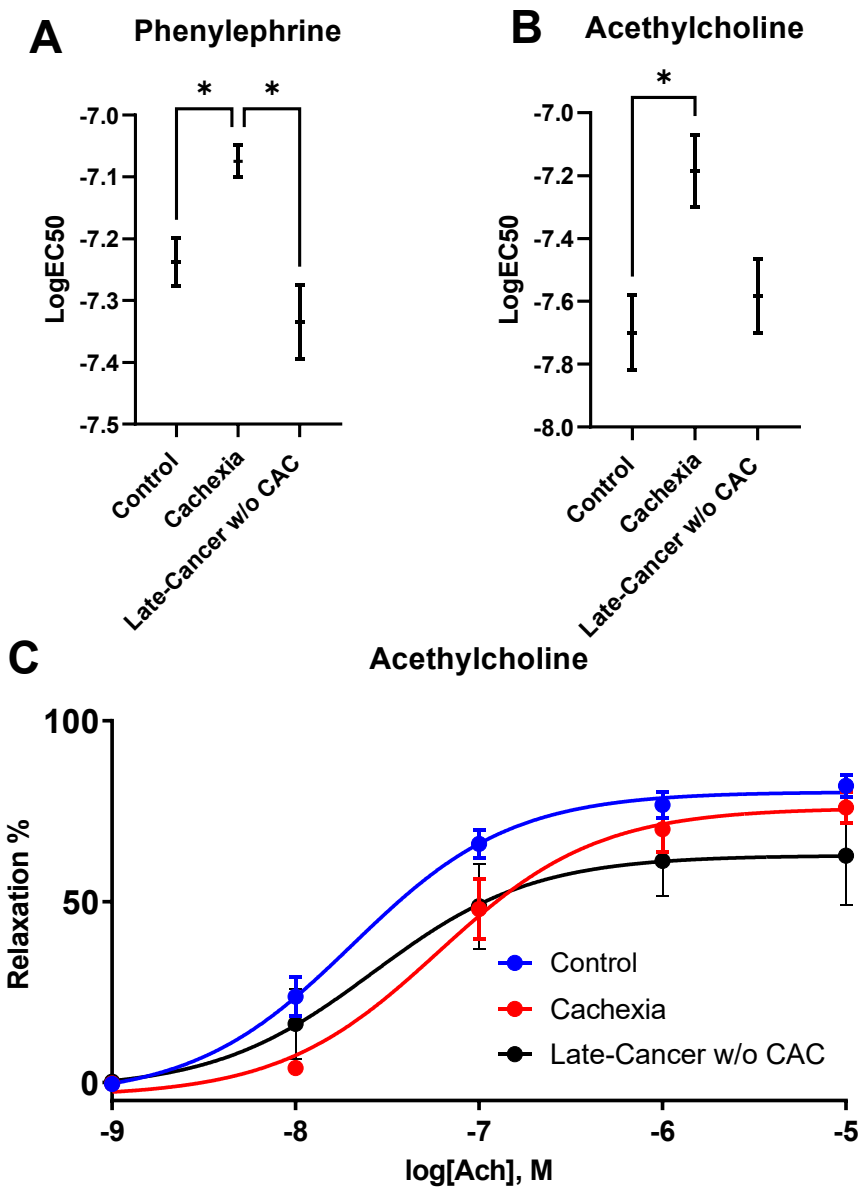

*Fig 9: A) Changes of LogEC50 Phenylephrine in cachectic animals. B) Changes of LogEC50 Acetylcholine in cachectic mice compared to control mice. C) Trend of decreasing vasodilatation in tumor bearing mice with less maximum reached relaxation to Ach 10^{-5} M compared to the control and cachexia group. Mean±SEM, n=8 Control, n=4 Pre-Cachexia, n=4 Early-Cancer w/o CAC, n=4 Cachexia, n=4 Late-Cancer w/o CAC, *p<0.05.*

ACE activity

The ACE activity in lung tissue lysate showed a trend to increase in both tumor bearing groups 8-10 days after the tumor cells injection (Fig 10). Interestingly, ACE activity levels in lungs show a tendency towards decreaseing at the later time point, but its level shows are still higher than in the controls (Fig 10). ACE not only converts angiotensin and acts on the renin–angiotensin–aldosterone system (RAAS), recent studies presented a connection to inflammatory processes, fibrosis and to cardiac remodeling [40, 41].

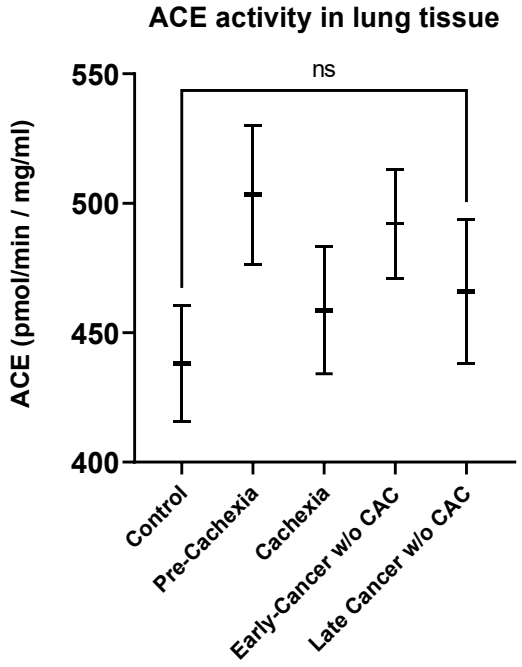

Fig 10: ACE activity measured in Lung tissue, no significant changes. Mean±SEM, n=11 Control, n=11 Pre-Cachexia, n=11 Early-Cancer w/o CAC, n=12 Cachexia, n=10 Late-Cancer w/o CAC.

Western Blot

BAG3 and HSP70 are suspected to be involved in cardiac remodeling, heart failure, inflammatory processes and fibrotic changes in cardiac tissue [6-9]. The protein expression of BAG3 and HSP70 was assessed by Western immunoblots. Both proteins expression were significantly decreased in LV tissue samples (late time point) in tumor bearing mice in comparison to controls (Fig 11 A and B). Additionally, BAG3 showed elevated values in early tumor bearing mice.

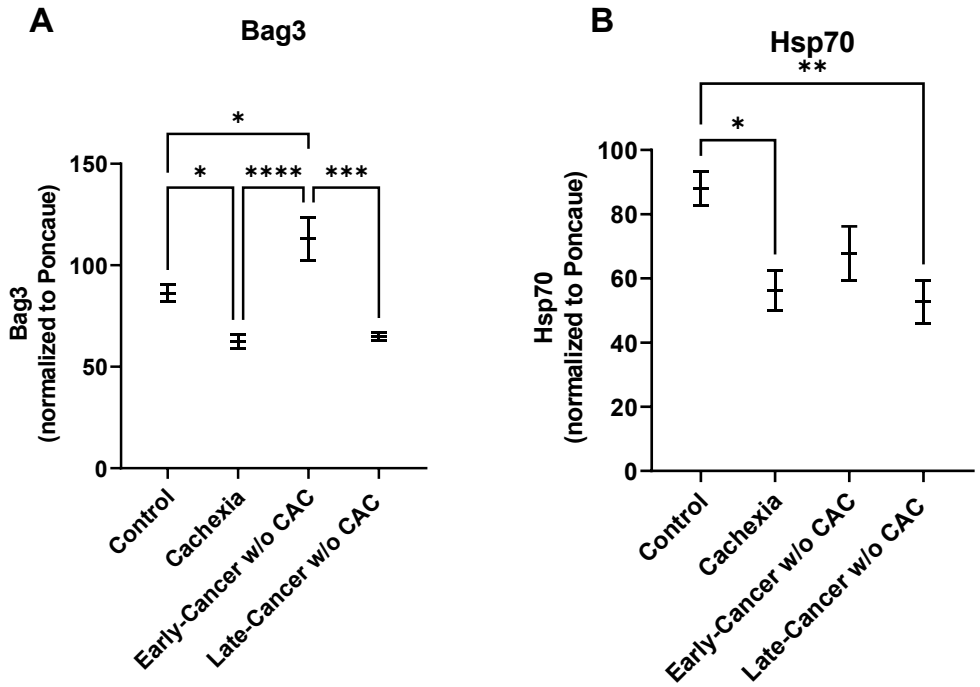

*Fig 11: A) B) Protein expression levels of BAG3 and HSP70 in cardiac tissue samples normalized to Poncause staining. Mean±SEM, n=10 Control, n=5 Early-Cancer w/o CAC, n=5 Cachexia, n=5 Late-Cancer w/o CAC, *p<0.05,**p<0.01,***p<0.001, ****p<0.0001.*

RT-qPCR

Expression of IL-1β, ACE 1, TLR-4, eNOS, VCAM and ICAM was assessed by RT-qPCR in lung isolated endothelial cells. Interestingly, mRNA levels of IL-1β was markedly increased in mice with cachexia (Fig 12). Generally, IL-1β, is a proinflammatory cytokine and marker of cancer cachexia progression [42]. Expression of inflammatory adhesive molecules (Vascular cell adhesion protein ,VCAM; intercellular adhesion molecule, ICAM) were not changed. ACE1 and Toll like receptor 4 (TLR-4) expression was also unaffected. Furthermore, endothelial nitric oxide synthase (eNOS) expression was unchanged among the groups.

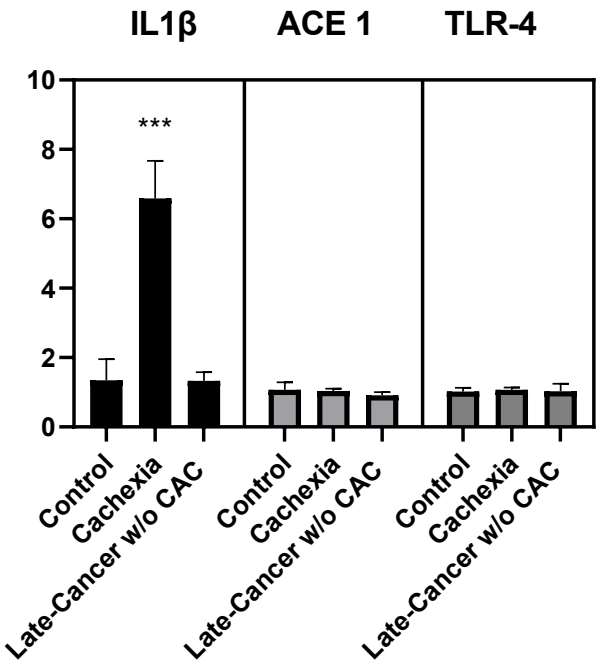

*Fig 12: Geneexpression in lung ECs of interleucin 1β (IL1b), ACE1, and Toll like receptor 4 (TLR-4). High expression of IL1b in cachectic animals compared to non-cachectic and control animals, fold change of >5. Mean±SEM, n=5 Control, n=5 Cachexia, n=5 Late-Cancer w/o CAC, ***p<0.001.*

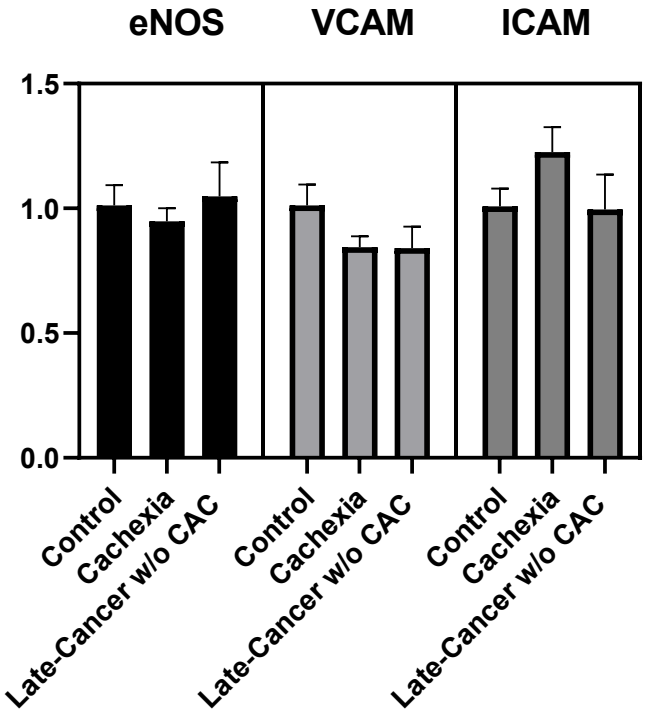

Fig 13: No changes in geneexpression in Lung EC of endothelial nitric oxide synthase (eNOS), vascular cell adhesion protein (VCAM), and intercellular adhesion molecule (ICAM). Mean±SEM, n=5 Control, n=5 Cachexia, n=5 Late-Cancer w/o CAC.

Histology

Masson-Goldner staining of mid-papillary heart area to identify fibrotic areas in heart slices. We observed no fibrotic area in non-cachectic animals, nor in cachectic mice in the late or early stage.

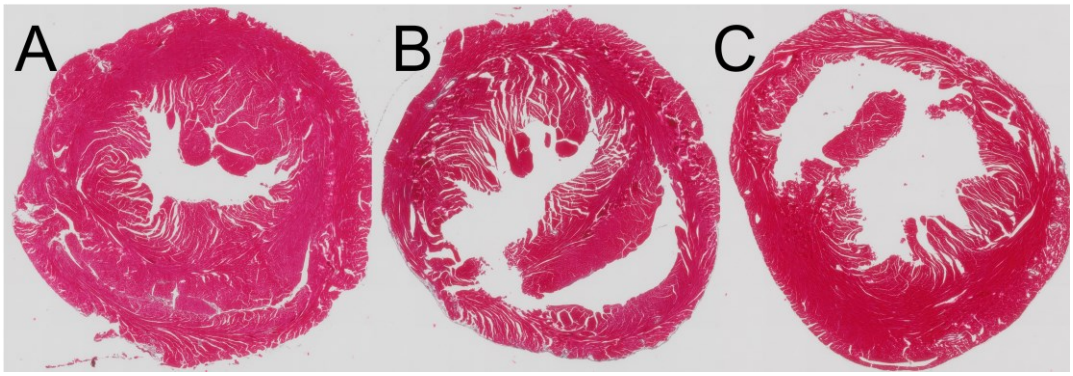

Fig 14: Representative histological pictures of Masso-Goldner staining at late time point of A) Cachectic mice B) Tumor bearing mice C) Control mice. No evidence of fibrosis.

Discussion

New findings

- Heart function seems to be unaffected in the early stage of tumor bearing mice but changed contractility, left ventricular systolic pressure, and diastolic function in the late stage of tumor bearing mice.
- Ejection fraction declined already in the early stage of tumor bearing mice.
- BAG3 and HSP70 expression were markedly decreased and associated with the cardiac dysfunction
- Vascular stiffness increased in tumor bearing mice

Cachexia progression

Mice were injected with IL-6 mRNA silenced C26 cells with, when compared to C26 cells treated mice there was no significant sign of cachexia. This was in line with previous findings [23]. Generally, IL-6 signaling in muscle tissue leads to wasteful metabolism via a mechanism involving STAT-3 and NF-κB pathways and the induction of ubiquitin-proteasome degradation and autophagy [43]. Despite, we did not measure IL-6 in this study, the loss of fat tissue and muscle tissue in cachectic animals compared to the other groups was significant. Interestingly, the total heart weight did not show any differences between the groups, suggesting organ/tissue-specific changes. In contrast, previous studies have demonstrated that tumor breading mice also shows cardiac atrophy and a reduction in LV mass [44, 45]. The discrepancies between our findings and those may be explained by the severity of models, numbers of cell injected or tumor size. Additionally, the early and late time point was based on previous studies [2]. Accordingly, 10 days after the respective protocols of injection, we observed a slight change in body weight, which is a marker of pre cachectic state (Fig 3).

At the end of the followup period (20 days), the size of the tumor significantly increased in comparison to the pre-cachetic stage. There was no difference in tumor size between the cancer groups (Fig 4). Next to body weight, muscle mass and fat deposit, we also characterized blood cells as well as their distrubtions. This is in line with previous preclinical and clinical findings [46-51]. The changes in Lymphocytes, Monocytes, and Granulocytes numbers and percentages within the blood reflects cancer and cachexia as well. Non-cachectic tumor bearing mice did also show a similar but attenuated pattern in the relative distribution of leukocytes. The organ weight of the spleen in cachectic animals, pre and late state, was markedly increased compared to control animals, suggesting a massive inflammatory character of cachexia. Tumor bearing mice without cachexia did show some increase in spleen weight too, this can certianly be explained by pro-inflammatory effects at a late stage of cancer. Of importance, based on the findings of Aulino *et al.* [52], the splenomegaly is a host response to C26 cell-injection. Nevertheless, we observed a significant interaction between cachexia and splenomegaly

Mechanistically, it is still unclear whether IL-6 acts as a trigger or mediator involved in the development of cachexia-associated splenomegaly. Neutrophil-to-lymphocyte ratio (NLR), is a known progression marker in oncology and surgical oncology, it serves as an indicator for systematic inflammation caused by tumors [39]. In our study, NLR was markedly increased in cachectic mice even at an early time point, while non-cachectic mice showed an elevation only in late stage (Fig 4), a connection to cancer-cachexia is already known [53, 54] and [46] an elevation of NLR even at an early stage in tumor bearing mice was found. This finding demonstrates and suggests that the inflammatory changes are already occurring early in the cachectic stage.

Cardiovascular complications

A recent clinical study demonstrated that the presence of cancer is independently associated with alterations of cardiac chamber size and function in patients with breast cancer or lymphoma prior to cardiotoxic cancer therapy exposure [55]. Consistently, other studies also demonstrated that localized tumors could affect heart function and result in cardiac dysfunction and fibrosis in tumor-bearing mice, making the heart more vulnerable to functional abnormalities in advanced stages of cancerous disease. The severity and relevance of CV risk vary widely depending on cancer type and cancer treatment regimens. Therefore, we aimed to clarify whether the presence of tumors or cachexia plays a dominant role in the development of cancer associated cardiovascular dysfunction in mice.

Hemodynamic changes

Changes in hemodynamic performance were observed in transthoracic echocardiography (Fig 5) and with the in vivo measurement by a pressure catheter (Fig 6). In Brief, our findings showed mostly a cachexia independent alteration of cardiac function like a decreased systolic pressure in the late vs early stage. Contractility was significantly reduced in cachectic animals compared to controls, in the other groups no significant changes were visible. Furthermore, diastolic function was also attenuated in the late group when compared to early stage animals. This is also reflected in the pressure time index, which additionally takes systolic duration and mean ventricular pressure

into account. Pressure time index was significantly reduced in late cachectic animals compared to early cachectic animals, non-cachectic animals only showed a non-significant trend. Moreover, our echocardiographic analysis showed differences in ejection faction, which is significantly reduced in comparison to control animals in all groups expect non-cachectic early stage animals (Fig 5). LVEDP was increased significantly in late tumor bearing mice, cachectic animals showed a trend towards increased LVEDP but there is no significant change (Fig 7). We did not find a hemodynamic parameter that is only cachexia specific and did not show similar trends in non-cachectic animals. Based on our findings, cachexia worsens some cardiac alterations that can be observed in tumor bearing mice but is not the main force behind it.

Vascular changes

There is evidence that some anti-neoplastic agents specifically target the vasculature to inhibit angiogenesis and tumor growth. For example, angiogenesis inhibitors, which can lead to increased vascular rarefaction, stiffness, resistance, and thrombosis even in non-cancer tissue such as the heart [56]. Additionally, the direct effect of cancer therapy on cardiomyocytes has been substantially investigated in comparison with the endothelium [57] and it is assumed to be crucial for the development of cardiovascular disease. However, the endothelium is the physiological gatekeeper of cardiomyocytes and also experiences the direct effects of radio- or chemotherapeutics.

In order to assess the impact of cancer on the development of vascular (dys)function, we isolated aorta segments and determined vascular function using a wire myograph. Our study for the first time demonstrated and dissected the impact of cancer and cancer cachexia on vascular relaxation and stiffness. Interstingly, vascular stiffness already increased at an early time point in mice with cancer cachexia (Fig 8). However, we did not aim to investigate the underling signalling mechansims, it is likely that changes of the vessel elastic properties contribute to the stiffening [13].

Additionally, endothelial funtion was assessed by dose-respone to ACh induced relaxation in isolated aortic rings. Concentration of ACh at which the reduction in force during dilation of a blood vessel is half the maximum value (EC50) was

signifcantly increased (shift) in cachectic animals, sugessting endothelial cell dysfunction (Fig 9). Several mechanisms, including oxidative stress, inflammation and changes in metabolism largely contribute to endothelial cell damage and dysfunction [58, 59].

These mechanisms are also known to link cancer and cancer cachexia. Therefore, we next investigated the expression of pro-inflammatory and cell adhesion markers in isolated lung endothelial cells.

In brief, we isolated endothelial cells from the lung tissue because it is realtive easy to receive a high number of cells as described previously [37]. There was no difference between mRNA expression of endothelial nitric oxide synthase (eNOS) (Fig 13) among the groups. Toll-like receptor 4 (TLR4), a possible target for cancer cachexia, is known to be upregulated in muscle tissue, macrophages, and adipocytes, which induces a release of proinflammatory molecules that may cause systematic inflammation associated with cachexia [60]. Nevertheless, TLR4 expression is not changed in endothelial cells, which indicates that other signalling mechanisms are leading to endothelial dysfunction, e.g. oxidative stress or inflammation. Angiotensin converting enzyme 1, not only a major player in the RAAS pathway also contributes to inflammatory processes and vascular dysfunction [40, 41]. Despite, we observed a tendency of increased ACE 1 activity in lung tissue, this was not associated with a expression elevation of ACE 1.

Interleukin 1β, is a well-established marker for the progession of cancer cachexia as well as an mediator for systematic inflammation [42]. Its expression in lung endothelial cells was significantly increased in cachectic mice when compared to control and non-cachectic animals. The elevation of Interleukin 1β in cachectic mice certainly contributes to the increase in vascular permeability [61], oxidative stress may partially explain the vascular endothelial dysfunction. The mRNA expression of cell adhesion molecules such as VCAM and ICAM did not show any differences between the groups.

ACE1 activity

Activation of the RAAS causes skeletal muscle wasting and weakness [62], it as well largely contributes to adverse cardiac remodeling [63]. We tested the hypothesis that in the upregulation of ACE 1 activity is associated with the loss of muscle and cardiovascular complications in our mouse model. We observed

a tendency towards to increased ACE 1 activity in lung tissue within tumor bearing mice when compared to the control group (Fig 10). Interestingly, the elevation of ACE 1 was more pronounced in the early stage of cancer. Additionally, ACE 1 activity in serum, kidney, and spleen tissue was assessed, but did not show any significant changes between the groups. Further studies are warranted to clarify whether ACE inhibitor or Ang II 1 receptor blockers limit the progression of cardiovascular complication in cancer patients.

BAG3 and HSP70

The cardiac dysfunctions that occur in cancer patients are primarily due to a catabolic shift in metabolic homeostasis, resulting in the aggravation of the proteolysis of the cardiac myocytes. This process is facilitated by inflammation and immune modulation via various cytokines such as IL-6, IL-1, TNFα as well as mitochondrial dysfunction, resulting in inadequate energy production and the accumulation of an excess number of reactive oxygen species [8, 64]. Moreover, the contractile filament dysfunction and abnormal expression of proteins are controled by autophagy and stabilized sarcomere may also contribute to contractile dysfunction [65]. BCL-2–associated athanogene 3 and Heat shock protein 70 are highly expressed in the myocardium. They have multiple functions intracellularly, including cellular protein quality control [8, 33, 34]. Additionally, there is increasing body of evidence that dysregulation of BAG3 in the myocardium plays a causative role in the progression of heart failure [66]. Since myofibrillar dysregulation is often present in cardiac cachexia, we hypothesized that cancer-canchexia also affect myofibrillar organization. In our studies, we did not assess cardiac contractile protein expression, but we found that BAG3 expression was markedly declined in tumor bearing mice hearts (late time point). This was associated with a massive decline in LV systolic pressure and LVEF. BAG3 is not only a co-chaperon with heat shock proteins but also associated with hypertrophy and cardiomyopathy, this is known from loss of function mutations which lead to a cardiomyopahtic phenotype in humans[33, 36]. Furthermore, BAG3 contributes to the stability of the cardiac sarcomere through regulation of filamin and by binding to CapZ [7]. Interestingly, BAG3 expression was even increased at an early time point in mice without cancer-associated cachexia.

Generally, misfolded proteins are toxic to cardiomyocytes and are directly contributing to the common accumulation which is found in heart failure [67]. One of the critical classes of proteins in protecting the heart against these threats are molecular chaperones, including the HSP70. However, HSP70 expression in cardiac tissue declined even in non-cachectic animals at the early time points. Additionally, there was no difference between cachectic and non-cachectic groups in respect to HSP70. This result suggests that cancer but not cancer cachexia plays a crucial role in the dysregulation of HSP70 in heart tissue from tumor bearing mice. Further studies are warranted to clarify the upstream signaling resulting in both HSP70 and BAG3 dysregulation in cardiac tissue in mice with cancer. Additionally, therapeutic targeting of BAG3 considering its complexity in cancer and heart disease [65] may alleviate cancer-associated moycardial contractile dysfunction.

Conclusion

We showed for the first time cachexia independent and dependent cardiac alterations in tumor bearing mice. Both systolic and diastolic dysfunctions were progressed in tumor bearing mice. The progression of cardiac contractile dysfunction was associated with a decline in BAG3 and Hsp70 in tumor-bearing mice, suggesting changes of BAG3/Hsp 70 signalling may be a critical component as well as target. In addition, BAG3 and HSP70 expression were markedly decreased and associated with the cardiac dysfunction. In contrast, inflammatory response in isolated lung endothelial cells and endothelial dysfunction was more pronoucned in mice with cancer cachexia.

Limitation

To reduce the burden of the used animals and ethical consideration, 20 days post injection was defined as endpoint (late stage). First, we did not observe smaller hearts in cachectic animals as previously stated in other publications using the identical animal model [13]. Of note, in our study the tumor size was significantly smaller (> 1.5 g), in previous studies the avarage size was 3-4 g. The size of tumor largerly depends on the total number of C26 cells which were used. Despite that, we observed a clear sign of cachexia, namely reduction in

skeletal muscle and fat deposit, we did not observe cardiac atrophy. Second, we used segments of aorta and assessed vascular function. Eventhough, the results are promising and confirmed the endothelial dysfunction, in order to conclude wheter cancer and cachexia initiate endothelial dysfunction, we need to isolate small diameter coronary arteries and perform the vascular reactivity assessment by using a pressure myograph system.

1. Chang, H.-M., et al., *Cardiovascular Complications of Cancer Therapy: Best Practices in Diagnosis, Prevention, and Management: Part 2.* Journal of the American College of Cardiology, 2017. **70**(20): p. 2552-2565.
2. Tian, M., et al., *Cardiac alterations in cancer-induced cachexia in mice.* International Journal of Oncology, 2010. **37**(2).
3. Petruzzelli, M. and E.F. Wagner, *Mechanisms of metabolic dysfunction in cancer-associated cachexia.* Genes & Development, 2016. **30**(5): p. 489-501.
4. Lena, A., A.J.S. Coats, and M.S. Anker, *Metabolic disorders in heart failure and cancer.* ESC Heart Failure, 2018. **5**(6): p. 1092-1098.
5. Feldman, A.M., et al., *BAG3 regulates contractility and Ca2+ homeostasis in adult mouse ventricular myocytes.* Journal of Molecular and Cellular Cardiology, 2016. **92**: p. 10-20.
6. Kimura, K., et al., *Overexpression of human BAG3P209L in mice causes restrictive cardiomyopathy.* Nature Communications, 2021. **12**(1).
7. Knezevic, T., et al., *BAG3: a new player in the heart failure paradigm.* Heart Failure Reviews, 2015. **20**(4): p. 423-434.
8. Martin, T.G., et al., *Pharmacological inhibition of BAG3-HSP70 with the proposed cancer therapeutic JG-98 is toxic for cardiomyocytes.* Journal of Cellular Biochemistry, 2021.
9. Jia, P., et al., *Different roles of BAG3 in cardiac physiological hypertrophy and pathological remodeling.* Translational Research, 2021. **233**: p. 47-61.
10. Nabel, E.G., *Cardiovascular Disease.* New England Journal of Medicine, 2003. **349**(1): p. 60-72.
11. *Cancer*. 2022 03.02.2022 [cited 2022 06.02.2022]; Available from: https://www.who.int/news-room/fact-sheets/detail/cancer.
12. Musolino, V., et al., *Cardiac expression of neutrophil gelatinase-associated lipocalin in a model of cancer cachexia-induced cardiomyopathy.* ESC Heart Failure, 2019. **6**(1): p. 89-97.
13. Shum, A.M.Y., et al., *Proteomic profiling of skeletal and cardiac muscle in cancer cachexia: alterations in sarcomeric and mitochondrial protein expression.* Oncotarget, 2018. **9**(31): p. 22001-22022.
14. Avraham, S., et al., *Early Cardiac Remodeling Promotes Tumor Growth and Metastasis.* Circulation, 2020. **142**(7): p. 670-683.
15. Argilés, J.M., et al., *Inter-tissue communication in cancer cachexia.* Nature Reviews Endocrinology, 2019. **15**(1): p. 9-20.
16. Anker, S., W. Steinborn, and S. Strassburg, *Cardiac cachexia.* Annals of Medicine, 2004. **36**(7): p. 518-529.
17. Coats, A.J.S., *Origin of symptoms in patients with cachexia with special reference to weakness and shortness of breath.* International Journal of Cardiology, 2002. **85**(1): p. 133-139.
18. Kalantar-Zadeh, K., et al., *Why cachexia kills: examining the causality of poor outcomes in wasting conditions.* Journal of Cachexia, Sarcopenia and Muscle, 2013. **4**(2): p. 89-94.
19. Okoshi, M.P., et al., *Heart Failure-Induced Cachexia.* Arquivos Brasileiros de Cardiologia, 2013.
20. Petruzzelli, M., et al., *A Switch from White to Brown Fat Increases Energy Expenditure in Cancer-Associated Cachexia.* Cell Metabolism, 2014. **20**(3): p. 433-447.
21. Dewys, W.D., et al., *Prognostic effect of weight loss prior tochemotherapy in cancer patients.* The American Journal of Medicine, 1980. **69**(4): p. 491-497.
22. Thivat, E., et al., *Weight change during chemotherapy changes the prognosis in non metastatic breast cancer for the worse.* BMC Cancer, 2010. **10**(1): p. 648.

23. Strassmann, G., et al., *Evidence for the involvement of interleukin 6 in experimental cancer cachexia.* Journal of Clinical Investigation, 1992. **89**(5): p. 1681-1684.
24. WEIDLE, U.H., et al., *Interleukin 6/Interleukin 6 Receptor Interaction and its Role as a Therapeutic Target for Treatment of Cachexia and Cancer.* Cancer Genomics - Proteomics, 2010. **7**(6): p. 287-302.
25. Zhang, D., et al., *Association of IL-6 gene polymorphisms with cachexia susceptibility and survival time of patients with pancreatic cancer.* Ann Clin Lab Sci, 2008. **38**(2): p. 113-9.
26. Weiner, R.B. and A.L. Baggish, *Exercise-Induced Cardiac Remodeling.* Progress in Cardiovascular Diseases, 2012. **54**(5): p. 380-386.
27. Kehat, I. and J.D. Molkentin, *Molecular Pathways Underlying Cardiac Remodeling During Pathophysiological Stimulation.* Circulation, 2010. **122**(25): p. 2727-2735.
28. Shum, A.M.Y., et al., *Cardiac and skeletal muscles show molecularly distinct responses to cancer cachexia.* Physiological Genomics, 2015. **47**(12): p. 588-599.
29. Belury, M., *Evidence for cardiac atrophic remodeling in cancer-induced cachexia in mice.* International Journal of Oncology, 2011.
30. Zheng, Y., et al., *Pay attention to cardiac remodeling in cancer cachexia.* Supportive Care in Cancer, 2016.
31. Wysong, A., et al., *NF-κB Inhibition Protects against Tumor-Induced Cardiac Atrophy in Vivo.* The American Journal of Pathology, 2011. **178**(3): p. 1059-1068.
32. Hinch, E.C.A., et al., *Disruption of pro-oxidant and antioxidant systems with elevated expression of the ubiquitin proteosome system in the cachectic heart muscle of nude mice.* Journal of Cachexia, Sarcopenia and Muscle, 2013. **4**(4): p. 287-293.
33. Myers Valerie, D., et al., *The Multifunctional Protein BAG3.* JACC: Basic to Translational Science, 2018. **3**(1): p. 122-131.
34. Inomata, Y., et al., *Bcl-2-associated athanogene 3 (BAG3) is an enhancer of small heat shock protein turnover via activation of autophagy in the heart.* Biochemical and Biophysical Research Communications, 2018. **496**(4): p. 1141-1147.
35. Seclì, L., et al., *Blocking Extracellular Chaperones to Improve Cardiac Regeneration.* Frontiers in Bioengineering and Biotechnology, 2020. **8**.
36. Liu, L., et al., *Advances in the role and mechanism of BAG3 in dilated cardiomyopathy.* Heart Failure Reviews, 2021. **26**(1): p. 183-194.
37. Osmanagic-Myers, S., et al., *Endothelial progerin expression causes cardiovascular pathology through an impaired mechanoresponse.* Journal of Clinical Investigation, 2018. **129**(2): p. 531-545.
38. Livak, K.J. and T.D. Schmittgen, *Analysis of Relative Gene Expression Data Using Real-Time Quantitative PCR and the 2−ΔΔCT Method.* Methods, 2001. **25**(4): p. 402-408.
39. Ying, H.-Q., et al., *The prognostic value of preoperative NLR, d-NLR, PLR and LMR for predicting clinical outcome in surgical colorectal cancer patients.* Medical Oncology, 2014. **31**(12).
40. Simões E Silva, A.C. and M.M. Teixeira, *ACE inhibition, ACE2 and angiotensin-(1□7) axis in kidney and cardiac inflammation and fibrosis.* Pharmacological Research, 2016. **107**: p. 154-162.
41. Turner, A.J. and N.N. Nalivaeva, *Angiotensin-converting enzyme 2 (ACE2): Two decades of revelations and re-evaluation.* Peptides, 2022. **151**: p. 170766.
42. Fogelman, D.R., et al., *A predictive model of inflammatory markers and patient-reported symptoms for cachexia in newly diagnosed pancreatic cancer patients.* Supportive Care in Cancer, 2017. **25**(6): p. 1809-1817.
43. Narsale, A.A. and J.A. Carson, *Role of interleukin-6 in cachexia.* Current Opinion in Supportive & Palliative Care, 2014. **8**(4): p. 321-327.
44. Tian, M., et al., *Cardiac alterations in cancer-induced cachexia in mice.* Int J Oncol, 2010. **37**(2): p. 347-353.

45. Cosper, P.F. and L.A. Leinwand, *Cancer Causes Cardiac Atrophy and Autophagy in a Sexually Dimorphic Manner.* Cancer Research, 2011. **71**(5): p. 1710-1720.
46. Pessini, P.G.D.S., et al., *Hematological reference values and animal welfare parameters of BALB/C-FMABC (Mus musculus) inoculated with Ehrlich tumor kept in the vivarium at ABC Medical School.* Animal Models and Experimental Medicine, 2020. **3**(1): p. 32-39.
47. Richards, D.M., J. Hettinger, and M. Feuerer, *Monocytes and Macrophages in Cancer: Development and Functions.* Cancer Microenvironment, 2013. **6**(2): p. 179-191.
48. Toor, S., et al., *Increased levels of circulating and tumor-infiltrating granulocytic myeloid cells in colorectal cancer patients.* Frontiers in Immunology, 2016. **7**.
49. Prokhorova, I., et al., *Influence of metformin, sodium dichloroacetate and their combination on the hematological and biochemical blood parameters of rats with gliomas C6.* Experimental oncology, 2018. **40**: p. 205-210.
50. Sanchez-Salcedo, P., et al., *The neutrophil to lymphocyte and platelet to lymphocyte ratios as biomarkers for lung cancer development.* Lung Cancer, 2016. **97**: p. 28-34.
51. Michaelis, K.A., et al., *Establishment and characterization of a novel murine model of pancreatic cancer cachexia.* Journal of Cachexia, Sarcopenia and Muscle, 2017. **8**(5): p. 824-838.
52. Aulino, P., et al., *Molecular, cellular and physiological characterization of the cancer cachexia-inducing C26 colon carcinoma in mouse.* BMC Cancer, 2010. **10**(1): p. 363.
53. Xu, C., et al., *Significance of the Neutrophil-to-Lymphocyte Ratio in p16-Negative Squamous Cell Carcinoma of Unknown Primary in Head and Neck.* Frontiers in Oncology, 2020. **10**.
54. Barker, T., et al., *An elevated neutrophil-to-lymphocyte ratio associates with weight loss and cachexia in cancer.* Scientific Reports, 2020. **10**(1).
55. Labib, D., et al., *Effect of Active Cancer on the Cardiac Phenotype: A Cardiac Magnetic Resonance Imaging-Based Study of Myocardial Tissue Health and Deformation in Patients With Chemotherapy-Naïve Cancer.* Journal of the American Heart Association, 2021. **10**(9).
56. Lenneman, C.G. and D.B. Sawyer, *Cardio-Oncology.* Circulation Research, 2016. **118**(6): p. 1008-1020.
57. Zhang, K., et al., *Paclitaxel accelerates spontaneous calcium oscillations in cardiomyocytes by interacting with NCS-1 and the InsP3R.* Journal of Molecular and Cellular Cardiology, 2010. **49**(5): p. 829-835.
58. Münzel, T., et al., *Impact of Oxidative Stress on the Heart and Vasculature.* Journal of the American College of Cardiology, 2017. **70**(2): p. 212-229.
59. Little, P.J., et al., *Endothelial Dysfunction and Cardiovascular Disease: History and Analysis of the Clinical Utility of the Relationship.* Biomedicines, 2021. **9**(6): p. 699.
60. Mccarty, M.F., S. Iloki-Assanga, and L.M.L. Lujany, *Nutraceutical targeting of TLR4 signaling has potential for prevention of cancer cachexia.* Medical Hypotheses, 2019. **132**: p. 109326.
61. Puhlmann, M., et al., *Interleukin-1β induced vascular permeability is dependent on induction of endothelial Tissue Factor (TF) activity.* Journal of Translational Medicine, 2005. **3**(1).
62. Murphy, K.T., et al., *Inhibition of the renin-angiotensin system improves physiological outcomes in mice with mild or severe cancer cachexia.* International Journal of Cancer, 2013. **133**(5): p. 1234-1246.
63. Gonzalez, A.A., L.G. Navar, and M.C. Prieto, *Renin-Angiotensin System Along the Nephron and its Role in Hypertension.* New Aspects of the Renin Angiotensin System in Cardiovascular and Renal Diseases, 2016: p. 138.
64. Wu, W., et al., *Hsp22 Deficiency Induces Age-Dependent Cardiac Dilation and Dysfunction by Impairing Autophagy, Metabolism, and Oxidative Response.* Antioxidants, 2021. **10**(10): p. 1550.

65. Kirk, J.A., J.Y. Cheung, and A.M. Feldman, *Therapeutic targeting of BAG3: considering its complexity in cancer and heart disease.* Journal of Clinical Investigation, 2021. **131**(16).
66. Maffioli, P., et al., *Detection of sieric BAG3 in patients affected by cardiovascular diseases: State of art and perspectives.* Journal of Cellular Biochemistry, 2022. **123**(1): p. 54-58.
67. Diteepeng, T., F. Monte, and M. Luciani, *The long and winding road to target protein misfolding in cardiovascular diseases.* European Journal of Clinical Investigation, 2021. **51**(5).

Supplements

Zusammenfassung

Hintergrund

Krebspatienten leiden oft an kardiovaskulären Komplikationen wie Herzversagen, die mit einer hohen Inzidenz der Mortalität einhergehen. Es ist unbekannt, ob krebs oder die miteinhergehende Kachexie die Treiber des Herzversagens sind. Diese Arbeit legt den Fokus auf BCL-2–associated athanogene 3 (BAG3), und Hsp70 und ihre Rolle in krebs induzierten Herzversagen.

Methoden

Colon-26 Adenokarzinomzellen (C26; n=22) mit als auch ohne IL-6 (C26 shIL-6; n=22) wurden 10-11 Wochen alten männlichen BALB/c Mäusen subkutan injiziert. Die Kontrollgruppe wurde ohne Zellen behandelt(PBS; n=8). Herzfunktion wurde beurteilt mittels Echokardiografie als auch via invasiver hämodynamischer Messmethoden jeweils 10 und 20 tage nach der Injektion. Des Weiteren wurde die Expression von BAG3 und Hsp70 per Western blot ermittelt.

Resultate

Die C26 Gruppe zeigte deutliche Anzeichen von Kachexie mit einhergehenden Verlust von fett und Muskelgewebe ($p<0.05$,). Links ventrikuläre Auswurfs Anteil war reduziert in der frühen Phase der Kachexie $p<0.05$), in der späten Phase zeigten beide Gruppen eine signifikante Reduktion. Das hämodynamische Assessment zeigte eine Reduktion der linksventrikulären Systole und eine Erhöhung des end diastolischen drucks ($p<0.05$). Diese Änderungen gingen mit einer deutlichen Reduktion an BAG3 und Hsp70 im Herzgewebe einher.

Diskussion

Diese Studie zeigt zum ersten Mal, dass der krebs selbst eine signifikante rolle in der Maladaption des Herzens spielt bei Mäusen mit krebsinduzierter Kachexie. Das Voranschreiten der kontraktilen Dysfunktion war assoziierte mit einer Reduktion von BAG3 und Hsp70 in den untersuchten Mäusen. In diesem Kontext könnte BAG3/Hsp70 eine kritische Komponente darstellen